Optical emission spectroscopy of a plasma jet for biomedical applications

E. Martines[1], L. Zampieri[1], R. Barni[1], M. Cavedon[1], G. Zarate Segura[2], C. Riccardi[1]

[1] *Department of Physics "G. Occhialini", University of Milano-Bicocca, 20126 Milano, Italy*

[2] *Physics Section, Pontificia Universidad Católica del Perú, 15088 Lima, Perú*

Atmospheric pressure plasma jets operating at low power levels, typically with helium or argon as main gas, have become a major tool for the studies of biomedical plasma applications ("plasma medicine"). Biological effects are primarily induced by active chemical species produced within the plasma thanks to the dissociation of air molecules mixing with the plasma plume. A proper modelling of the complex chemistry taking place within the plasma requires a knowledge of the plasma parameters. While advanced diagnostic techniques can be used to deduce many of these properties, it is also of interest to have simple methods to make the same kind of estimation. One of the simplest diagnostic techniques which can be used is Optical Emission Spectroscopy (OES). However, an interpretation of OES requires a proper modelling of the balance between excited states excitation and decay processes, through what is known as a Collisional-Radiative Model (CRM). Several attempts have been made to write CRMs for atmospheric pressure argon plasmas [1,2,3,4]. However, these models tend to be exceedingly complex, involving not only many excited Ar states, but also ionization/recombination and excimers formation/decay. Here we present our work towards a barebone CRM model for atmospheric pressure Ar plasmas, capable of estimating the electron temperature and density from emission spectra in the optical range, and its application to spectra obtained for a low-power Ar plasma jet for biomedical applications.

The lowest energy levels of the Ar atoms are (in Paschen notation): the ground state $1s_1$, the four 1s excited states (two metastables, $1s_3$ and $1s_5$, and two resonant states, $1s_2$ and $1s_4$), and the ten 2p levels, labelled from $2p_{10}$ to $2p_1$ in increasing energy order. The optical transitions observed in the spectrum pertain to the decay of 2p levels to the excited 1s levels.

Our model describes the populations of: 1) the ground state; 2) the four 1s levels; 3) the ten 2p levels; 4) the 3d levels and the 2s levels, lumped into a single "3d+2s" level with average energy; 5) the 3p levels, lumped into a single "3p" level of average energy. Thus, a total of only 17 states are considered.

The populations n_x of the different levels are determined as the solutions of the following coupled equations, which assume stationary conditions:

$$\sum_{y \neq x} R_{y \to x} n_y - n_x \sum_{y \neq x} R_{x \to y} = 0.$$

where $R_{x\to y}$ represents the total transition rate from state x to state y. The processes considered for the transitions among these levels are: 1) excitation and decay by electron impact, 2) excitation and decay by impact with neutrals, 3) spontaneous emission. The optical thickness of the plasma, due to photon capture and re-emission, has been ignored. Thus, $R_{x\to y}$ represents the sum of the rate coefficients of the transitions from state x to state y due to the different processes, multiplied by the relevant densities: $R_{x\to y} = Q^e_{x\to y} n_e + Q^n_{x\to y} n_g + A_{x\to y}$ where the superscript 'e' indicates transitions due to electron impact, the superscript 'n' transitions due to impact with neutral atoms, the last term is Einstein coefficient for spontaneous decay, and n_e and n_g are the electron density and the density of neutral atoms. Normalizing all densities to n_g and assuming for n_g the ideal gas particle density at atmospheric pressure, only the ionization fraction $f_e = n_e/n_g$ remains as parameter. The rate coefficients for electron and neutral impact depend on the electron temperature T_e and the gas temperature T_g respectively: assuming T_g to be equal to the room temperature, only T_e remains as parameter, together with f_e.

Electron-impact reaction rates are evaluated from the BSR and the IST databases of cross-sections available in LXCat [5]. Spontaneous radiative decay rates are obtained from the NIST atomic spectra database. Atom-impact reaction rates are obtained from different sources: Chang and Setser for decays from 2p to 1s [6]; Nguyes and Sadeghi for 2p internal population mixing [7]; Zhu and Pu for higher levels [8]. For each process, the rate coefficient of the inverse process is obtained using the principle of detailed balance.

An example of the relative magnitude of the different terms in eq.1 is shown in fig.1, for the case T_e = 1.7 eV and $f_e = 2.1\times10^{-6}$, which corresponds to the actual conditions of the plasma

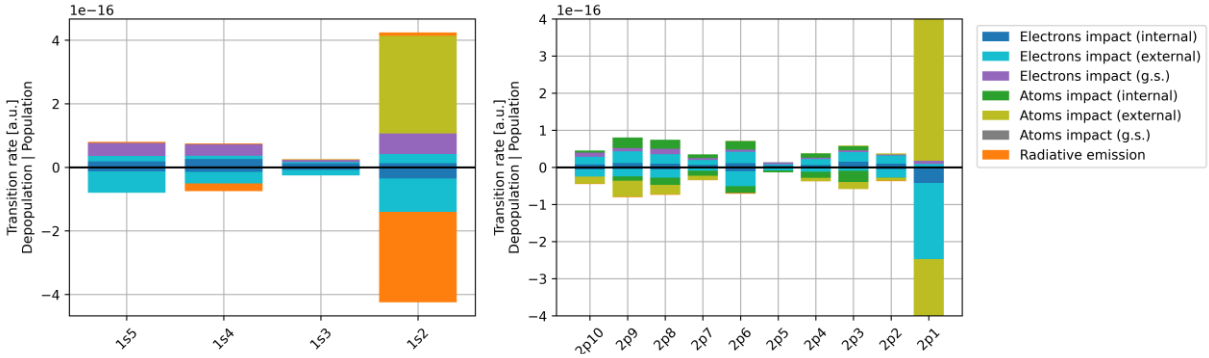

Fig. 1:Transition rates in the 1s and 2p multiplets, for T_e = 1.7 eV and $f_e = 2.1\times10^{-6}$

jet, as given by the fit described below. The positive values correspond to excitation rates, while the negative values give decay rates. Contrary to what happens in low-pressure plasmas, the role of radiative emission is negligible for 2p levels, and appears to be relevant only for $1s_2$ and, partially, for $1s_4$. On the contrary, both collisions with electrons and with neutral atoms play as important role, both in excitation and in de-excitation processes. Thus, including proper rates for atom collisions is essential to achieve a meaningful result.

Experiments were carried out using a plasma jet developed for biomedical applications. The jet consists of a central needle covered by a glass capillary surrounded by a glass nozzle (Ø 7.0 mm) with an external ground ring. Argon flows in the nozzle at approximately 2 slpm, and the needle is excited by 100 kHz, ~5 kVpp sinusoidal voltage.

Optical emission spectra were obtained using an Avantes AvaSpec-ULS4096CL-EVO compact spectrometer, capable of measuring spectra from 200 to 1100 nm with a resolution of 0.3 nm. The optical system consisted of a 6-mm diameter lens with 8.7 mm focal length, focused within the plasma jet, so that light from a spot with 0.5 mm diameter could be collected and sent to the spectrometer through an optical fibre. The measured spectra were calibrated using a calibration curve measured using a calibration lamp.

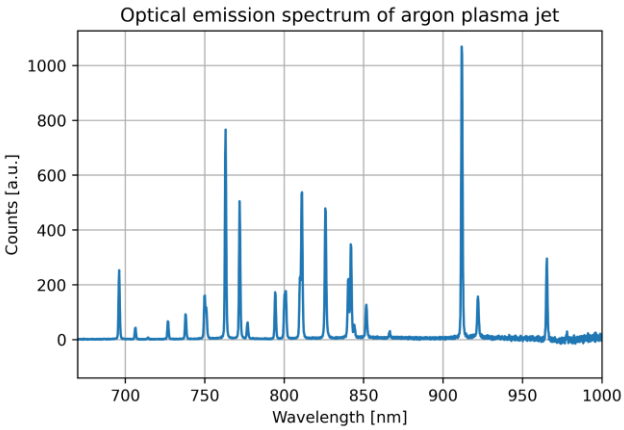

Fig. 2: Typical spectrum from the Ar plasma jet

An example of spectrum measured on the plasma jet is shown in fig.2. First, a consistency check was performed: since the emission on a line is proportional to the Einstein coefficient multiplied by the upper-level population density, it was checked that the ratios of the intensities of lines having the same upper level were equal to the ratios of the relevant Einstein coefficients. The line intensity was evaluated with a gaussian fit of the line shape, taking as intensity the area under the resulting gaussian curve.

For evaluating the plasma parameters, the χ^2 defined as

$$\chi^2 = \sum_x \frac{(n_x - AN_x)^2}{\sigma_{N_x}^2 + \sigma_{n_x}^2}$$

where n_x are the state densities resulting from the model and N_x are the experimental densities, with A a scaling constant which minimizes the χ^2 value. The obtained χ^2 was minimized against the two free parameters T_e and f_e. An important issue here is which lines to include in the χ^2. While in principle one might think that all detectable lines resulting from the decay of a 2p level should be included, some selection criteria were used. Partially overlapping lines (with peak distance less than 2 nm) were excluded. Furthermore, it was found that different sources report different branching ratios for atom-impact transitions $2p_9 \rightarrow 2p_{10}$ and $2p_9 \rightarrow 1s$. Considering that the $2p_{10}$ mainly decays towards 1s, this uncertainty in the cross sections only affects the estimated density of $2p_{10}$ level. Similarly, incongruence about the atom-impact population exchanges between the $2p_1$, $2p_2$ and $2p_3$ levels exists in the literature. Therefore, the population

distribution among these states is not reliable. Consequently, the selected levels for the fit are $2p_9$, $2p_8$, $2p_6$ and $2p_4$, for a total of eight transitions.

An example of fit is shown in fig.4. The optimization against the T_e and f_e parameters was performed in the 2D space, but here we show for simplicity only the cross-sections of the χ^2

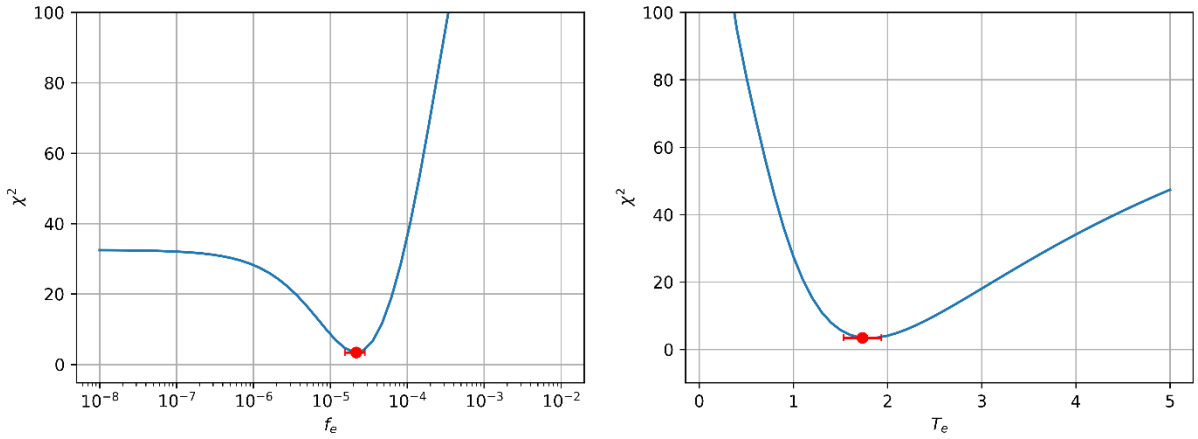

Fig. 3: χ^2 plotted as a function of T_e and f_e, with the optimizing values and their uncertainties marked in red.

surface along the two axes. The presence of a well-defined minimum is evident, which gives confidence on the result of the optimization. The resulting values of the two parameters are $T_e = 1.7 \pm 0.2$ eV and $f_e = (2.1 \pm 0.6)\times10^{-5}$. The uncertainties are estimated from the square roots of diagonal covariance matrix elements, in the assumption of uncorrelated variables, which is computed as $C \approx 2[H(f)]^{-1}$, where H(f) is the Hessian matrix of the f function [9].

Acknowledgements

The authors acknowledge COST Action CA20114-PlasTHER "Therapeutical Applications of Cold Plasmas", supported by COST (European Cooperation in Science and Technology).

This work was funded by the National Plan for NRRP Complementary Investments (PNC, established with the decree-law 6 May 2021, n. 59, converted by law n. 101 of 2021) in the call for the funding of research initiatives for technologies and innovative trajectories in the health and care sectors (Directorial Decree n. 931 of 06-06-2022) - project n. PNC0000003 - AdvaNced Technologies for Human-centrEd Medicine (project acronym: ANTHEM). This work reflects only the authors' views and opinions, neither the Ministry for University and Research nor the European Commission can be considered responsible for them.

References

[1] J. Vlcek, J. Phys. D: Appl. Phys. **22** 623 (1989)
[2] A. Bogaerts et al., J. Appl. Phys. **84**, 121 (1998).
[3] X.-M. Zhu and Y.-K. Pu, J. Phys. D: Appl. Phys **43**, 403001 (2010).
[4] A. Durocher-Jean, E. Desjardins and L. Stafford, Phys. Plasmas 26, 063516 (2019).
[5] O. Zatsarinny, Y. Wang and K. Bertschat, Phys. Rev. A 89, 022706 (2014).
[6] T. D. Nguyen and N. Sadeghi, Phys. Rev. A 18, 1388 (1978).
[7] R. S. F. Chang and D. W. Setser, J. Chem. Phys. **69**, 3885 (1978).
[8] X.-M. Zhu and Y.-K. Pu, J. Phys. D: Appl. Phys **43**, 015204 (2010).
[9] P. Bevington, Data Reduction and Error Analysis for the Physical Sciences, MgGraw-Hill.